Journal of Applied Mechanics and Technical Physics, Vol. 40, No. 6, 1999

TECHNIQUE FOR EXPERIMENTAL DETERMINATION OF THE TOTAL THRUST–AERODYNAMIC CHARACTERISTICS OF AIRCRAFT MODELS

A. V. Lokotko

UDC 533.6.011:605

A method of experimental determination of the force characteristics of nozzles (thrust, lift, and pitching moment) simultaneously with the aerodynamic characteristics of an aircraft model in a supersonic flow is proposed. The tests were conducted for a special methodical model, with equilibrium of the thrust and drag forces being reached. It is shown that the internal force characteristics of the nozzle and the drag of the model, as well as the effective lift and pitching moment (with account of propulsion), can be determined from the measured thrust of the propulsion simulator.

Introduction. The nearest prospect is the operation of flying vehicles in the range of hypersonic velocities in the air space. With increasing flight velocity, the shape of a flying vehicle is determined to a large extent by the significant increase in the entrance area of the inlet and the exit area of the reactive nozzle in the total mid-section. The so-called integral configuration is considered at present. In this case, the wing and the fuselage are united into a single lifting structure, which includes the elements of a powerplant located at the lower surface. The oblique forebody of the fuselage serves as a compression surface of the inlet, and the gas-jet expansion occurs near the oblique trailing surface. This integration allows one to decrease the mass parameters of the inlet and the nozzle and increase the effective lift-to-drag ratio of a flying vehicle by using the lift force generated by these elements [1].

A necessary stage in the design of all flying vehicles is the wind-tunnel studies of their models. However, the traditional methods, which deal mainly with the aerodynamic characteristics of the fuselage and disregard factors caused by propulsion, are little suitable for hypersonic velocities for two reasons. First, in the traditional approach where the propulsion effects are simulated only by flow reproduction on compression surfaces of the inlet in the presence of the engine-nacelle duct, significant base rarefaction is observed on the expanding surface of the duct near the tail part of the body. This rarefaction varies in a rather complex manner and strongly distorts the aerodynamic coefficients obtained. The introduction of the corresponding corrections into all components of the resultant force is rather complicated and labor-consuming and does not ensure the required accuracy. Second, the jet expansion near the base has a dramatic influence on the effective lift-to-drag ratio, aircraft balance, and effective thrust of the powerplant.

Thus, it is necessary to test the models of hypersonic flying vehicles in wind tunnels with mandatory simulation of propulsion and with account of the special features that affect the external flow. The corresponding criteria of modeling, which mainly refer to the range of moderate flight velocities, are well known (see, e.g., [2, 3]). Within the range of very high velocities, the influence of factors related to propulsion becomes commensurable with the acting aerodynamic forces and determines the efficiency of the configuration as a whole. Therefore, it is desirable to develop test techniques with more detailed dynamic modeling, in particular, in reaching equilibrium of the drag and thrust forces, which corresponds to the regime of steady

Institute of Theoretical and Applied Mechanics, Siberian Division, Russian Academy of Sciences, Novosibirsk 630090. Translated from Prikladnaya Mekhanika i Tekhnicheskaya Fizika, Vol. 40, No. 6, pp. 73–82, November–December, 1999. Original article submitted May 7, 1998; revision submitted July 16, 1998.

cruising flight. Dynamic interaction of the captured stream tube with the constructional elements is possible if the following dimensionless parameters are reproduced on the model: the relative area of the inlet entrance, the flow-turning angles and the throat area determining the degree of compression, the flow-rate coefficients depending on flight regimes, and the nozzle-thrust coefficient.

The reproduction of the nozzle thrust coefficient $c_{P_x} = P_x/(qS)$ with modeling of the nozzle geometry, i.e., the exhaust Mach number, requires conservation of the relative total pressure $\pi = p_{0,\text{noz}}/p_\infty$ and, as a consequence, the nozzle pressure ratio p_{noz}/p_∞. Here P_x is the longitudinal component of thrust, $q = (1/2)æp_\infty \text{M}^2$ is the dynamic pressure, S is the reference area, $p_{0,\text{noz}}$ is the total pressure in the model receiver, p_{noz} is the pressure at the nozzle exit, p_∞ is the free-stream pressure, æ is the ratio of specific heats, and M is the Mach number. The oblique tail part of the fuselage is, in essence, an asymmetric two-dimensional nozzle. The study of exhaust processes from these nozzles under conditions of interaction of the jet with the external flow and the associated interference phenomena is of significant interest.

The following method for wind-tunnel testing of the models of hypersonic flying vehicles is proposed.

1. The model is equipped with a propulsion simulator, which ensures the necessary thrust coefficient for given flow parameters at the inlet entrance. It is assumed that this simulator is a ducted engine nacelle equipped with an ejector (see, for example, [4]).

2. The model is mounted on a balance in the test section of the wind tunnel in a known manner. It is weighted in a supersonic external flow at different angles of attack to obtain a polar in the coordinates of effective (with account of propulsion) drag c_{xa} and lift c_{ya} coefficients, and also the pitching moment m_{za}.

3. In deriving this polar, the thrust of the propulsion simulator is varied at each fixed angle of attack. It is desirable to reach equilibrium of the drag and thrust forces (the measured resultant longitudinal force is $R_x = 0$). From the polars obtained, the specific impulses of the corresponding force components of an asymmetric nozzle are found by the method proposed below; after that, the effective aerodynamic coefficients are calculated.

The present paper is devoted mainly to a methodical justification of the proposed method of aerodynamic testing with the use of a special methodical model without an inlet. The tests were conducted at zero initial incidence. In addition, the test results are given for the same model equipped with a wing in the flow with $\text{M}_\infty = 6.11$, which were published earlier [5] but were processed again using the proposed technique. On the one hand, these results illustrate the method; on the other hand, they demonstrate some effects of interference of the jet and external flow upon their interaction near the wing surface.

Description of the Model and Test Conditions. The experiments were conducted in the T-313 supersonic wind tunnel of the Institute of Theoretical and Applied Mechanics, Siberian Division of the Russian Academy of Sciences with the test-section size 0.6 × 0.6 m for Mach numbers $\text{M}_\infty = 3.02, 4.03$, and 6.11 and Reynolds numbers $\text{Re} = 37 \cdot 10^6$, $54 \cdot 10^6$, and $9 \cdot 10^6$ m^{-1}.

A sketch of the model is shown in Fig. 1 (dimensions are given in millimeters). The model is a fuselage mounted on a knife-shaped strut, which is fixed on the beam of an external mechanical aerodynamic balance. A channel for supplying the working medium of the jet is made inside the strut; in our case, it was air. The model construction and the system for insulation of the model from the feeding pipeline are described in detail in [5, 6]. In the present experiments, the model was modified: the previously existing possibilities of replacing various model elements (nozzle and wing, and both can be located in direct and reverse positions) were supplemented by a possibility of changing the configuration of the nose part of the model: it can be pointed or blunted (Fig. 1, detachment in cross section A–A). This allowed us to vary the drag coefficient of the model. The aerodynamic coefficients were calculated for the mid-section area of the model $S = 0.008664$ m^2, and the pitching moment was calculated for a conventional mean aerodynamic chord $b_a = 0.1$ m.

Three types of nozzles were used. All of them had a rectangular cross section with the following exit parameters: height 60 mm and width 70 mm. One of the nozzles was a symmetric configuration (Fig. 1, view B), and the two other nozzles were asymmetric. The distance between the trailing edge and the cowl edge in the asymmetric nozzles was 120 mm. The symmetric nozzle and one asymmetric nozzle had the

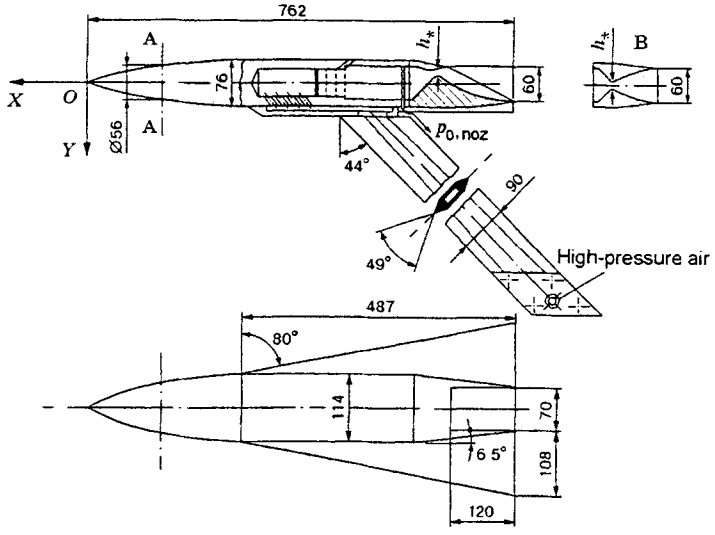

Fig. 1

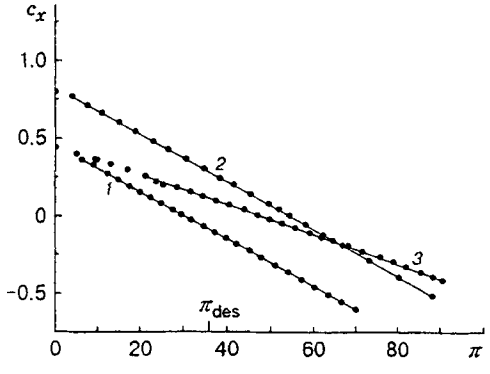

Fig. 2

throat height $h_* = 14.28$ mm and the degree of expansion 4.20. For the symmetric nozzle, the degree of expansion corresponded to the exhaust Mach number $M_{noz} = 2.99$. The second asymmetric nozzle used in experiments at $M_\infty = 6.11$ had $h_* = 8.65$ mm and the degree of expansion 6.94. One nozzle was chosen among similar available nozzles [7]; it was distinguished by the most developed separation phenomena on the external surface upon interaction of the exhausted jet with the incoming stream.

The nozzle contours were calculated by A. I. Rylov in accordance with results [8].

The pressure in the model receiver was measured by an MID-100 system with scannivalves that had an operating range of 0–0.6 MPa and an accuracy of 0.2% of the measurement limit. The force loads were measured by riders with accuracy about 0.1%.

Experimental dependences were approximated and the corresponding coefficients were calculated using a standard AXUM code.

Test Results. Figure 2 shows the dependences $c_x(\pi)$ obtained by testing the model without the wing in the regime with $M_\infty = 4.03$ for different variants of model equipment. Each point denotes a measurement result. The results are given for the symmetric nozzle and a pointed nose part of the model (curve 1), the symmetric nozzle and a blunted nose part (curve 2), and the asymmetric nozzle with $h_* = 14.28$ mm and a pointed nose part (curve 3). The dependences for the symmetric nozzle (curves 1 and 2) become strictly linear as π increases, beginning from the values $\pi_{lin} = 7$–8, and then cross the abscissa axis. For this nozzle,

TABLE 1

M	Type of the nose part	a_x	b_x	c'_{x0}	c_{pb}	c_{x0}	c_{P_x}	δ, %
3	Pointed	0.596 44	−0.027 90	0.554 55	−0.082 58	0.514 51	0.520 01	1.06
	Blunted	0.924 52	−0.027 76	0.879 77	−0.073 62	0.844 08	0.848 40	0.51
4	Pointed	0.464 41	−0.015 37	0.450 58	−0.025 68	0.438 13	0.422 23	3.63
	Blunted	0.838 53	−0.015 39	0.815 60	−0.031 86	0.800 15	0.796 16	0.50

the optimal or design exhaustion regime ($p_{\text{noz}} = p_\infty$) corresponds to $\pi_{\text{des}} = 36.18$, and the nozzle pressure ratio in the self-similar regime is $\pi_{\text{lin}}/\pi_{\text{des}} \cong 0.21$. At the point of intersection with the abscissa axis, the measured value of the longitudinal resultant force is $R_x = 0$, i.e., the drag is balanced by the thrust. The tangent of the slope of curves 1 and 2 can be defined as the ratio of the difference of two arbitrary values of the aerodynamic coefficients of the resultant longitudinal forces $c_{R_x}1$ and $c_{R_x}2$ to the difference of π_1 and π_2:

$$\tan\omega = \frac{c_{R_x}1 - c_{R_x}2}{\pi_1 - \pi_2} = \frac{[p_{0,\text{noz}}F_{\text{noz}}f(\lambda_{\text{noz}}) - p_\infty F_{\text{noz}} - X]_1 - [p_{0,\text{noz}}F_{\text{noz}}f(\lambda_{\text{noz}}) - p_\infty F_{\text{noz}} - X]_2}{qS[(p_{0,\text{noz}}/p_\infty)_1 - (p_{0,\text{noz}}/p_\infty)_2]}.$$

Here F_{noz} is the nozzle-exit area, $f(\lambda_{\text{noz}})$ is a gas-dynamic function, λ_{noz} is the velocity coefficient, and X is the longitudinal aerodynamic force.

Since $[p_\infty F_{\text{noz}}; X]_1 = [p_\infty F_{\text{noz}}; X]_2$, we have $\tan\omega = \Delta p_0 F_{\text{noz}} f(\lambda_{\text{noz}})/(qS\Delta\pi)$. This expression has the meaning of the specific impulse of the nozzle [9] represented as an aerodynamic coefficient. In the self-similar regime of exhaustion ($\lambda_{\text{noz}} = \text{const}$), we have $\tan\omega = \text{const}$, i.e., the dependence is a straight line, which is observed in the experiment.

Approximating the linear portions of the resulting dependences by straight lines of the form

$$y = a + bx, \tag{1}$$

we obtain $a \equiv c_{x0}$, $b \equiv \tan\omega$, and $x \equiv \pi$. Thus, the tangent of the slope of the straight lines is proportional to the coefficient of specific evacuated impulse of the nozzle.

We consider the coefficient a in more detail. On the one hand, a is the root of Eq. (1) for $x = \pi = 0$, i.e., the drag coefficient c_{x0} in a passive flow (without thrust). Obviously, in this case c_{x0} includes the base-drag forces. On the other hand, $a = \pi\big|_{c_{R_x}=0} \cdot \tan\omega = \pi p_{0,\text{noz}} F_{\text{noz}} f(\lambda_{\text{noz}})/(\pi qS)$ is the evacuated impulse (force) at reaching the drag–thrust equilibrium, which is written in the form of an aerodynamic coefficient. It is of interest to compare these two quantities, which can serve as a test of reliability of measurements. This comparison allows one also to evaluate c_{x0} of the model of a particular flying vehicle with a complex contour of the tail part avoiding the passive test with base-pressure measurement. For a symmetric nozzle, the experiments are mainly conducted for verification, since the base drag can be easily taken into account by measuring the base pressure. Writing an expression for the thrust force, we can compose an assumed equality

$$a - p_\infty F_{\text{noz}}/(qS) = c'_{x0} - c_{pb}F_{\text{noz}}/S, \tag{2}$$

where $c_{pb} = (p_b - p_\infty)/q$ is the base-pressure coefficient and p_b is the base pressure. Here and below, the prime denotes the value obtained in balance tests.

The left part of Eq. (2) is the thrust coefficient c_{P_x}, and the right part is the drag coefficient with elimination of the base-drag coefficient c_{xb}, i.e., $c_{x0} = c'_{x0} - c_{xb}$. Thus, Eq. (2) can be written in the following form:

$$c_{P_x} = c_{x0}. \tag{3}$$

It should be noted that the change in the model drag caused by mounting a pointed or blunted nose part leads to a strictly equidistant shift of the dependences $c_x(\pi)$; therefore, the accuracy of satisfaction of equality (3) is evaluated for both cases. The same effect is exerted on c_x by the strut, i.e., the presence of

TABLE 2

M	a_x	b_x	c'_{x0}	c_{P_x}
3	0.591 78	−0.017 29	0.560 64	0.515 36
4	0.458 66	−0.009 61	0.443 95	0.416 29

the strut does not affect the magnitude of the specific impulse. The measurement results for pointed and blunted nose parts of the model are listed in Table 1. Here and in the sequel, the coefficients a and b of the linear dependence of the form of (1) are marked by the subscripts of the corresponding force component. In Table 1, δ is the residual of the left and right parts of Eq. (3); it is mainly within 1%, but in one case it is 3.63%. This deviation is, apparently, related to the insufficient accuracy of base-pressure measurement: at a low level ($p_b \sim 3$ kPa), it was measured by a transducer designed for 0.6 MPa, as the pressure $p_{0,\text{noz}}$. In addition, the distance at which the pressure was measured was quite large (about 4 m); this required a long time of wind-tunnel operation, which was not always possible. In Table 1, the value $c_{pb} = -0.02568$ differs significantly from other values, which confirms the above assumption.

For the asymmetric nozzle with $h_* = 14.28$ mm (curve 3 in Fig. 2), the dependence has a significantly smaller slope. The value of the specific impulse is smaller by 38% than that for the symmetric nozzle with $h_* = 14.28$ mm. The values of the approximation coefficients and aerodynamic coefficients obtained in experiments with the asymmetric nozzle are listed in Table 2.

The experiments with the asymmetric nozzle demonstrate that it is possible to determine the drag coefficient of the model from the measured thrust without base-pressure measurements. Comparing the values of c_{P_x} (Table 2) with the values of c_{x0} (Table 1), we obtain a rather small difference, for example, for $M_\infty = 3.02$ and a pointed nose of the model, it is 0.16%. This means that the external contours of the symmetric and asymmetric nozzles are rather close, and we can determine c_{x0} for complex configurations from the measured thrust:

$$c_{x0} = \pi\Big|_{c'_x=0} \cdot \tan\omega - p_\infty F_{\text{noz}}/(qS).$$

We note that the value of c_{x0} calculated on the basis of thrust differs from that measured directly (without base-pressure measurement) by 8.1%.

We can also evaluate the reliability of the proposed measurement technique by determining the internal force characteristics of the symmetric nozzle ($\bar{I}'/\bar{I}_{\text{ideal}}$) using the formula

$$\bar{I}_{\text{ideal}} = I_{\text{ideal}}/(F_* p_{0,\text{noz}}) = [2/(æ+1)]^{1/(æ-1)} Z(\lambda_{\text{noz}}),$$

where F_* is the nozzle-throat area and $Z(\lambda_{\text{noz}})$ is a gas-dynamic function of the impulse. The value of the specific impulse coefficient $\bar{I}'$ based on the measurement results can be calculated by the formula $\bar{I}' = b_x qS/(F_* p_\infty)$.

For the present geometry of the nozzle, we have $\lambda_{\text{noz}} = 1.962$ and $\bar{I}_{\text{ideal}} = 1.5669$. In experiments, we obtained $\bar{I}'/\bar{I}_{\text{ideal}} = 0.9776$ and 0.9775 for $M_\infty = 3$ and 4, respectively. This ratio determined the level of perfection of the nozzle. The values obtained are typical of supersonic planar nozzles [10], which verifies the effectiveness of the method proposed.

The dependences $c_y(\pi)$ for $M_\infty = 3.02$ are plotted in Fig. 3 for symmetric and asymmetric nozzles with $h_* = 14.28$ mm mounted on the model with a pointed nose (curve 1 corresponds to the symmetric nozzle and curve 2 to the asymmetric nozzle). The lift force for a symmetric nozzle is changed by angular deformation of the model suspension under the action of thrust and drag forces, which was discussed in detail in [5]. The additional normal force Y_{err} that arises is an experimental error and should be taken into account. At the same time, there should be no deformation in the regime of equilibrium of longitudinal forces ($R_x = 0$), and the true angle of attack of the model should correspond to the initially established angle. For different manners of model suspension, deformations induced by the action of all components of the resultant force should be taken into account.

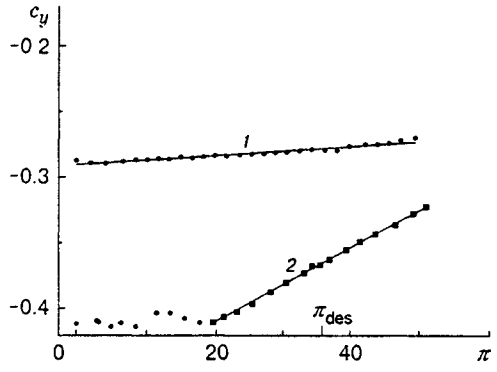

Fig. 3

TABLE 3

Configuration of the model	Nozzle and wing position	a_x	b_x	c_{x0}
Without wing	Direct	0.397 46	−0.004 18	0.3789
	Reverse	0.386 36	−0.004 19	0.3678
With wing	Direct	0.439 63	−0.004 22	0.4211
	Reverse	0.426 63	−0.004 16	0.4081

Two special features are observed for the asymmetric nozzle. First, with increasing π, the establishment of the self-similar regime begins significantly later than for the symmetric nozzle, which is particularly noticeable on the dependences $c_y(\pi)$ in contrast to $c_x(\pi)$: the beginning of the linear section corresponds to $\pi_{\text{lin}} \cong 20$. Second, the lift coefficient in the region of small π is significantly smaller for the model with the asymmetric nozzle than for the symmetric nozzle. This is related to propagation of the base pressure to the extended part of the nozzle. The loss of the lift force is compensated by jet exhaustion only at $\pi \cong 80$, and a further increase in c_y is observed with increasing π. This special feature depends on the angle of attack, as is shown in [5].

We consider the results of testing the model equipped with a wing and an asymmetric nozzle with $h_* = 8.65$ mm in a flow with $M_\infty = 6.11$, which were published in [5] and processed again in accordance with the present method.[1] In the present tests, we used the method for the direct and reverse positions of the nozzle and the wing, which allowed us to refine the estimates for the lift coefficient and moment characteristics in the absence and presence of the wing.

The approximation coefficients a_x and b_x for the linear dependences $c_x(\pi)$ and the values of c_{x0} calculated on the basis of the specific impulse are listed in Table 3. The values of c_{x0} for the model with a wing turned out to be higher than those for the model without the wing, which is quite natural. The noticeable difference in c_{x0} for the direct and reverse positions of the wing can be explained by interference interaction of the flow in the vicinity of the strut.

Figure 4 shows the dependences $c_y(\pi)$ for the model with the asymmetric nozzle with $h_* = 8.65$ mm for $M_\infty = 6.11$. Of primary importance here is the difference in the specific impulse along the normal axis in the presence and absence of the wing, which is the manifestation of the interference effects on interaction of the jet and the external flow. Curves 1 and 2 in Fig. 4 refer to the direct and reverse positions of the nozzle for the model without the wing, and curves 3 and 4 refer to the direct and reverse positions of the nozzle

[1]The tests were supported by AEROSPATIALE (France).

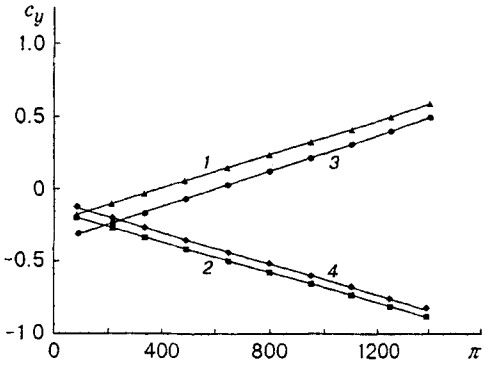

Fig. 4

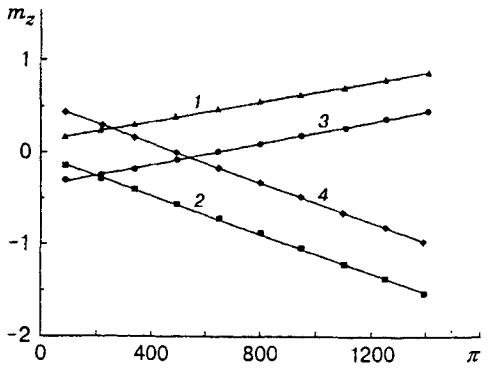

Fig. 5

and the wing for the winged model. To eliminate the errors induced by deformation of the model suspension, using results [4], we can write the following expressions for the coefficients b_y, which are the specific impulses along the normal axis:

$$b_y^- = |b_1| - [|b_1| - |b_2|]/2 \quad \text{or} \quad b_y^- = |b_2| + -[|b_1| - |b_2|]/2,$$

$$b_y^+ = |b_3| - [|b_3| - |b_4|]/2 \quad \text{or} \quad b_y^+ = |b_4| + [|b_3| - |b_4|]/2.$$

The superscripts plus and minus denote the model with and without the wing, respectively, and the subscripts 1–4 denote the corresponding number of the curve. These tests were performed for much higher values of π than those corresponding to $R_x = 0$; the errors of the induced force Y_{err} were quite significant and amounted to 4.7% for the model without the wing and 6.8% for the model with the wing; therefore, the account of these errors was necessary. As a result, we obtained $b_y^- = 5.52 \cdot 10^{-4}$ and $b_y^+ = 5.75 \cdot 10^{-4}$. Comparing these values for the model with and without the wing, we obtain a 4% gain in the specific impulse due to interference of the jet and the external flow near the wing surface. This value is lower than that reported previously (5%) [5], but it is more reliable, since the approximation coefficients were calculated on the basis of all the measurements. Thus, the method allows one to identify the interference effects due to interaction of the exhausted jet and the external flow.

The total impulse coefficient b_I can be represented as the resultant of specific impulses along the OX and OY axes and expressed in terms of the approximation coefficients of the corresponding straight lines:

$$b_I = \sqrt{\left(\frac{\Delta c_x}{\Delta \pi}\right)^2 + \left(\frac{\Delta c_y}{\Delta \pi}\right)^2} = \sqrt{b_x^2 + b_y^2}.$$

The slope of the total impulse vector is $\varphi = \arctan(b_y/b_x)$, it is $\varphi = 7.52°$ for the model without the wing and $\varphi = 7.75°$ for the model with the wing.

The pitching moment $m_z(\pi)$ relative to the moment axis of the balance for the model without and with the wing for the direct and reverse positions of the nozzle with $h_* = 8.65$ mm and the wing for $M_\infty = 6.11$ is shown in Fig. 5. The notation is the same as in Fig. 4. The general pattern is similar to the dependences $c_y(\pi)$, but the symmetry of the slopes of the curves relative to the horizontal axis is significantly violated, which is related to the absence of intersection of the model centerline with the moment axis of the balance. The distance between these axes is the ordinate of the balance axis y_0 in the model-fixed coordinate system. This quantity should be known (taking into account the subsequent development of the method with full aerodynamic testing of winged models), but its determination prior to experiment in the case of using unusual systems of model suspension (in particular, a pylon strut) is difficult because of deformation of the suspension elements under the action of aerodynamic forces and thrust, and difficulties in conducting the corresponding spatial measurements in the test section of the wind tunnel. As a result, the moment axis of the balance "floats" in the coordinate space of the model during the tests. The method proposed allows one to determine the position of the moment axis of the balance in the model-fixed coordinate system.

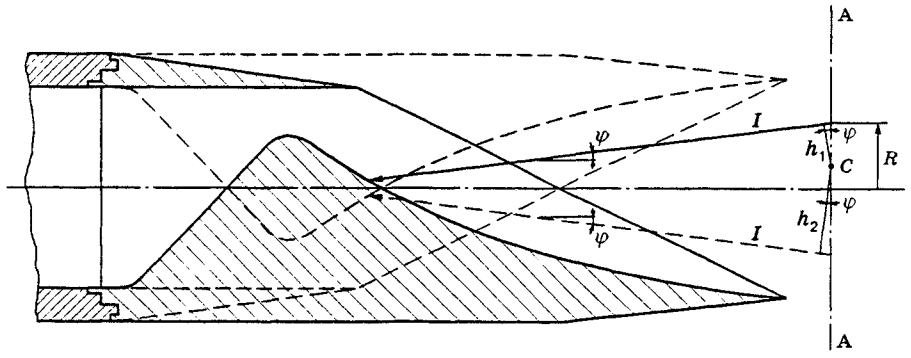

Fig. 6

The expressions for the arms of the total impulse vector induced by jet injection (in fractions of the mean aerodynamic chord) have the following form in the model-fixed coordinate system for the direct and reverse positions of the nozzle:

$$h_1 = b_{mz1}/b_I, \qquad h_2 = b_{mz2}/b_I.$$

Here b_{mz1} and b_{mz2} are the tangents of the slope of the moment dependences.

For the known slope of the total impulse vector φ and longitudinal distance to the plane A–A, which contains the moment axis of the balance C, we can easily find the spatial position of the balance axis relative to the model (the solid curves in Fig. 6 refer to the direct position of the nozzle and the dashed curves to the reverse position). If we turn the nozzle around the model centerline, the total impulse vector $\boldsymbol{I}$ will draw a circle of radius $R = [(h_1 + h_2)\cos\varphi]/2$ in the plane A–A. The total impulse includes the induced normal force Y_{err}. In this case, the contribution of this force to the total impulse is about 0.08%; nevertheless, it can cause significant errors in the moment by acting on the arm $l_{Y_{\text{err}}}$. Writing the equations for moments acting in the direct and reverse positions of the nozzle in the form $M_1 = Ih_1 + Y_{\text{err}}l_{Y_{\text{err}}}$ and $M_2 = -Ih_2 + Y_{\text{err}}l_{Y_{\text{err}}}$ and passing to the tangents of the slope of the moment dependences, we obtain

$$h_1 - h_2 = (b_{mz1} - b_{mz2})/b_I. \tag{4}$$

In the present experiments, we have $h_1 = 12.76$ mm and $h_2 = -24.93$ mm, and from formula (4) we obtain $h_1 - h_2 = 37.69$ mm. These distances are in agreement with the physical pattern of the acting forces. Then, we can find the ordinate of the balance axis $y_0 = R - h_1\cos\varphi$.

The moment $Y_{\text{err}}l_{Y_{\text{err}}}$ is determined by testing the model without the jet and varying the angle of attack [5]. Obviously, the action of this moment leads to a parallel shift of the moment dependences.

Thus, the proposed approach serves as a basis for development of the test technique with determination of the joint thrust-aerodynamic forces of the model and powerplant. Subsequent studies can be related to unification of the method proposed and the traditional techniques of aerodynamic testing of winged models with variation of the angle of attack and also with known methods (for example, [11]) that allow minimization of the effect of suspension devices.

The author is grateful to A. I. Rylov for calculation of nozzle contours, to A. M. Kharitonov for supporting this work, and to T. Bonnefond for partial financing of the studies.

REFERENCES

1. R. I. Kurziner, *Reactive Engines for High Supersonic Flight Velocities* [in Russian], Mashinostroenie, Moscow (1989).
2. V. B. Vologodskii, "Conditions of modeling of an air flow around a flying vehicle with an operating reactive engine," in: *Collection of papers of the Riga Institute of Civil Aircraft Engineering* [in Russian], No. 1, Riga (1960).
3. N. A. Dubov, "Simulation of interaction of the powerplant and the fuselage of a flying vehicle in wind-tunnel tests," *Tr. TsAGI*, No. 1818 (1976).
4. A. V. Lokotko and L. A. Trifonov, USSR Inventor's Certificate No. 1212149, MKI G 01 M 9/00, "Simulator of the powerplant of the model of a supersonic flying vehicle," No. 3764797, Submitted 10.15.85, Bul. No. 16, Priority 07.13.84.
5. A. V. Lokotko, "Method for determination of the force characteristics of asymmetric nozzles in a supersonic external flow," *Teplofiz. Aeromekh.*, **4**, No. 4, 325–337 (1997).
6. A. V. Lokotko, "Method for determination of internal force characteristics of the model in a supersonic external flow," *Sib. Fiz.-Tekh. Zh.*, No. 1, 53–60 (1992).
7. V. N. Zudov, A. V. Lokotko, and A. I. Rylov, "Numerical and experimental investigation of two-dimensional nozzles," AIAA Paper No. 96-3141 (1996).
8. A. I. Rylov, "Analysis of optimal asymmetric nozzles with account of moment characteristics," *Izv. Akad. Nauk SSSR, Mekh. Zhidk. Gaza*, No. 4, 103–108 (1988).
9. U. G. Pirumov and G. S. Roslyakov, *Gas-Dynamics of Nozzles* [in Russian], Nauka, Moscow (1990).
10. G. N. Lavrukhin and G. I. Poleshchuk, "Plane nozzles in integral aircraft configurations," *Obzor TsAGI*, No. 586 (1980).
11. V. S. Zuenko, A. V. Lokotko, and A. A. Rafaélyants, "Method of balance tests on a fin sting," in: *Proc. III All-Union School on the Methods of Aerophysical Research* (Novosibirsk, July 1982), Inst. Theor. Appl. Mech., Sib. Div., USSR Acad. Sci., Novosibirsk (1982), pp. 36–39.